Journal of Inorganic Biochemistry 119 (2013) 54–64

Contents lists available at SciVerse ScienceDirect

Journal of Inorganic Biochemistry

journal homepage: www.elsevier.com/locate/jinorgbio

Exploring the DNA binding/cleavage, cellular accumulation and topoisomerase inhibition of 2-hydroxy-3-(aminomethyl)-1,4-naphthoquinone Mannich bases and their platinum(II) complexes

Amanda P. Neves [a,1], Michelle X.G. Pereira [b], Erica J. Peterson [a], Ralph Kipping [a], Maria D. Vargas [c], Floriano P. Silva-Jr [b], J. Walkimar M. Carneiro [c], Nicholas P. Farrell [a,*]

[a] Department of Chemistry, Virginia Commonwealth University, 1001 West Main Street, Richmond, VA 23284, USA
[b] Laboratório de Bioquímica de Proteínas e Peptídeos, Fundação Oswaldo Cruz, Instituto Oswaldo Cruz, Av. Brasil, 4365, Manguinhos, Rio de Janeiro, RJ, CEP: 21040-360, Brazil
[c] Instituto de Química, Universidade Federal Fluminense, Campus do Valonguinho, Centro, Niterói, RJ, CEP: 24020-141, Brazil

ARTICLE INFO

Article history:
Received 12 June 2012
Received in revised form 8 October 2012
Accepted 8 October 2012
Available online 15 October 2012

Keywords:
Naphthoquinone
Pt^{2+} complexes
DNA binding
DNA strand breaks

ABSTRACT

Several chlorido and amino Pt^{2+} complexes of 2-hydroxy-3-(aminomethyl)-1,4-naphthoquinone Mannich bases **HL** exhibiting moderate to high cytotoxicity against cancer cell lines were studied in order to investigate their modes of DNA binding, *in vitro* DNA strand breaks, mechanism of topoisomerase (Topo I) inhibition and cellular accumulation. DNA model base studies have shown that complex **1a** [Pt(**HL1**)Cl_2] was capable of binding covalently to 9-ethylguanine (9-EtG) and 5′-GMP. ^{1}H NMR and mass spectrometry studies have shown that both chlorides were substituted by 9-EtG ligands, whereas 5′-GMP was able to replace only one chlorido ligand, due to steric hindrance. The chlorido Pt^{2+} complexes [Pt(**HL**)Cl_2] highly accumulate in prostate (PC-3) and melanoma (MDA-MB-435) cell lines, being able to induce DNA strand breaks *in vitro* and inhibit Topo I by a catalytic mode. On the other hand, the free 2-hydroxy-3-(aminomethyl)-1,4-naphthoquinones **HL** and the amino Pt^{2+} complexes [Pt($\mathbf{L}^-$)$(NH_3)_2$]NO_3 neither cause DNA strand breakage nor exhibit strong DNA interaction, nevertheless the latter were also found to be catalytic inhibitors of Topo I at 100 μM. Thus, coordination of the Mannich bases **HL** to the "$PtCl_2$" fragment substantially affects the chemical and biophysical properties of the pro-ligands, leading to an improvement of their DNA binding properties and generating compounds that cleave DNA and catalytically inhibit Topo I. Finally, the high cytotoxicity exhibited by the free (uncomplexed) 2-hydroxy-3-(aminomethyl)-1,4-naphthoquinones might be associated with their decomposition in solution, which is not observed for the Pt^{2+} complexes.

1. Introduction

Natural and synthetic quinone derivatives have been widely investigated for cancer therapy [1–3]. Many drugs containing a quinone moiety, such as *Mitomycin C* and *Doxorubicin* have received clinical approval for cancer treatment [1,4,5]. In general, the biological activity of quinones derives from the ability of the quinone moiety to accept one or two electrons to form semiquinone and cathecol radicals. These species are re-oxidized by molecular oxygen (O_2) generating highly reactive oxygen species (ROS), such as superoxide anion radical, which play a key role in mutagenesis and carcinogenesis [6,7]. The production of ROS has been commonly related to DNA strand break production and to the oxidative stress observed in cells [8,9]. Especially for polycyclic quinonoid compounds, such as naphthoquinones and anthraquinones, their DNA interactions (intercalation or alkylation) might also contribute to their cytotoxicity. Moreover, naphthoquinones have been shown to act as topoisomerase inhibitors, an activity that may also be involved in their cytotoxic mechanism [10–12].

We have been working extensively on the design of novel naphthoquinone derivatives [11–15], including Mannich bases and their Cu^{2+} complexes [16,17], which present interesting bactericidal activity [17]. The Mannich bases derived from 2-hydroxy-1,4-naphthoquinone (lawsone) were first synthesized in the 1940s and their antimalarial and molluscicidal activities have been investigated [18–21]. Recently, we have reported the synthesis and cytotoxicity of unprecedented Pt^{2+} complexes of 2-hydroxy-3-(aminomethyl)-1,4-naphthoquinone Mannich bases (Scheme 1), with high to moderate activity against several tumor cell lines [22] (SI (Supplementary Information), Table S1). The search for novel Pt-based drugs [23–25] has been a priority since the discovery of cisplatin [26]. Most Pt^{2+} complexes act similarly to cisplatin, through the binding of the [Pt$(amine)_2]^{2+}$ moiety to the DNA, forming covalent adducts that inhibit replication and

* Corresponding author. Tel.: +1 804 828 6320; fax: +1 804 828 8599.
E-mail address: npfarrell@vcu.edu (N.P. Farrell).
[1] Present address: Departamento de Química, Universidade Federal Rural do Rio de Janeiro, BR-465, Km 7 Seropédica, RJ, CEP: 23890-000, Brazil.

0162-0134/$ – see front matter © 2012 Elsevier Inc. All rights reserved.
http://dx.doi.org/10.1016/j.jinorgbio.2012.10.007

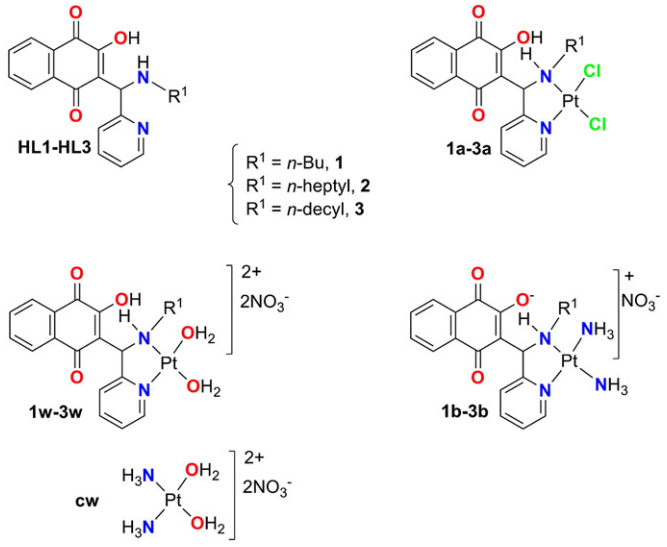

Scheme 1. Chlorido **1a–3a**, aqua **1w–3w** and amino **1b–3b** Pt^{2+} complexes of 2-hydroxy-3-(aminomethyl)-1,4-naphthoquinones **HL1–HL3** studied in this work.

transcription, causing cellular apoptosis and necrosis [27]. However, other Pt^{2+} derivatives such as the trinuclear BBR3464 and TriplatinNC show different DNA binding modes with long-range interstrand crosslinks and non-covalent interactions – electrostatic and hydrogen bonding – respectively [28]. Lately, the attachment of biologically relevant molecules to Pt^{2+}, *e.g.* intercalators [29], tamoxifen [30] and porphyrins [31] have been successfully explored as an alternative to combine two different active fragments in one molecule. In the present work, we describe a series of biophysical and cellular studies on the previously published [22] 2-hydroxy-3-(aminomethyl)-1,4-naphthoquinone Pt^{2+} complexes (**1a–3a**, **1b–3b**) and the respective pro-ligands **HL1–HL3** (Scheme 1). We have also investigated the interactions between the *cis*-[Pt(**HL1**)Cl_2] **1a** complex and the DNA model bases 9-ethylguanine (9-EtG) and 5′-GMP. We show that the incorporation of Pt^{2+} into 2-hydroxy-3-(aminomethyl)-1,4-naphthoquinones causes significant changes in the biophysical properties of the pro-ligands, strongly affecting their cytotoxicity and mechanism of action.

2. Experimental section

2.1. Materials and methods

Reagents and solvents were used as purchased without further purification. Calf thymus DNA (CT-DNA) and ethidium bromide (EtdBr) were obtained from Sigma-Aldrich. 5′-GMP (Aldrich) was employed as a disodium salt. Supercoiled plasmid DNA (pUC19) was isolated from *E. coli* strain XLI-blue with the use of Qiagen DNA purification kits. All stock solutions of the investigated compounds were prepared by dissolving the powdered materials in appropriate amounts of DMF or DMSO. Deionized double distilled water and analytical grade reagents were used throughout. CT-DNA stock solution was prepared by dissolving the solid material in $NaClO_4$ buffer 10 mM. Then, the solution was dialyzed for 24 h at 4 °C. The resulting somewhat viscous solution was clear and particle-free. The CT-DNA concentration in terms of nucleotides L^{-1} was determined spectrophotometrically by employing an extinction coefficient of 6600 M^{-1} cm^{-1} (nucleotide)$^{-1}$ at 260 nm [32]. The stock solution was stored at 5 °C until it was used. EtdBr was dissolved in 10 mM of phosphate buffer (pH 7.4) and its concentration was determined assuming a molar extinction coefficient of 5600 L mol^{-1} cm^{-1} at 480 nm [33]. Buffers used and their abbreviations are: phosphate buffers (10 mM phosphate, 50 mM NaCl, pH 7.4 and 2 mM phosphate, pHs 7.0 and 5.8) and TAE (40 mM Tris, 20 mM acetic acid, 1 mM EDTA, pH 8.0).

^{1}H NMR spectra were recorded on a Varian Mercury 300 MHz NMR spectrometer in DMF-d_7 (*N*,*N*-dimethylformamide-d_7) and mixture of D_2O/DMF-d_7 (3:1). Chemical shifts were referenced to 3-trimethylsilylpropionic acid, sodium salt, used as internal standard. ^{195}Pt NMR spectra were recorded on a Varian Mercury NMR spectrometer using a 10 mm broadband probe. ^{195}Pt spectra were referenced to $Na_2[PtCl_6]$. The frequency for ^{195}Pt nuclei was set at 64.32 MHz. Mass spectra were obtained in a Micromass QTof-2 instrument. Samples, whose final concentrations were 1 μg/μL, were dissolved in 1:1 methanol:water and injected using direct infusion method with the flow rate of 0.5μL/min.

2.2. Synthesis

The 2-hydroxy-3-(aminomethyl)-1,4-naphthoquinones **HL1–HL3** derivatives, chlorido **1a–3a** and amino **1b–3b** Pt^{2+} complexes were synthesized as described in the literature [22]. The DMF solutions (5 mM) of compounds [Pt(**HL1-3**)$(DMF)_2$]$(NO_3)_2$ and [Pt$(NH_3)_2$$(DMF)_2$]$(NO_3)_2$, were obtained by reacting a 100 mM $AgNO_3$ solution (0.4 mL, 0.04 mmol) with **1a–3a** (0.02 mmol) and with cisplatin (6 mg, 0.02 mmol), respectively, in DMF (3.6 mL) at 50 °C for 24 h. The resulting AgCl precipitate was filtered off. [Pt(**HL1-3**)$(H_2O)_2$]$(NO_3)_2$ **1w–3w** and [Pt$(NH_3)_2(H_2O)_2$]$(NO_3)_2$ **cw** were obtained by dilution of the DMF solutions with water to a final concentration of 95:5 (water:DMF). The water solution (5 mM) of [Pt(**HL1**)$(H_2O)_2$]$(NO_3)_2$ **1w** was also prepared using the same procedure above, except for the use of H_2O instead of DMF, for the gel mobility shift assays.

2.3. Molecular modeling

Density functional calculations were carried out using the Gaussian03W molecular orbital package [34]. Geometries were fully optimized using the B3LYP functional [35] with the LANL2DZ basis set [36]. The initial geometry was taken from the crystallographic structure of **1a** [22] after replacement of one or two chlorine ions by the 9-EtG base.

2.4. DNA model base studies

2.4.1. Reaction of *cis*-[Pt(**HL1**)Cl_2] **1a** with 9-ethylguanine (9-EtG)

For the ^{1}H NMR, *cis*-[Pt(**HL1**)Cl_2] (5 mg, 0.0083 mmol) was allowed to react with 9-EtG (3 mg, 0.0166 mmol) in an NMR tube using 0.7 mL of DMF-d_7 at room temperature. A 6-fold excess of **1a** and 9-EtG was used for ^{195}Pt NMR in 2 mL of DMF-d_7. ^{1}H and ^{195}Pt NMR spectra were recorded over time. After 72 h, an aliquot of the solution from the NMR tube was evaporated and re-suspended in a mixture of MeOH/H_2O (1:1) in order to perform a mass spectrometry analysis.

2.4.2. Reaction of *cis*-[Pt(**HL1**)Cl_2] **1a** with 5′-GMP

The reaction of *cis*-[Pt(**HL1**)Cl_2] (6 mg, 0.01 mmol) and 5′-GMP (8.2 mg, 0.02 mmol) was carried out in the NMR tube in a mixture of D_2O/DMF-d_7 (3:1, total 1 mL) at room temperature. A 4-fold excess of **1a** and 5′-GMP was used for ^{195}Pt NMR in D_2O/DMF-d_7 (3:1, total 2 mL). ^{1}H and ^{195}Pt NMR were recorded over time and mass spectrometry was performed after analysis of an aliquot from the NMR tube after 72 h of reaction.

2.5. Measurement of melting curves

100 μM nucleotides of CT DNA were incubated with compounds **HL1**, **1w**, **1b** and **cw** at various binding ratios (r_i = [Drug]/[nucleotides] = 0, 0.01, 0.03, 0.05, 0.075 and 0.1) in 0.01 M $NaClO_4$ with 5% DMF for 72 h in the dark. The data were recorded on a JASCO V-550

UV-visible (UV–vis) spectrophotometer by measuring the absorbance at 260 nm. Temperature was varied from 40 to 98.5 °C increasing at the rate of 0.5 °C per min. Melting points were estimated as the temperature when 1/2 of absorbance increase was reached.

2.6. Fluorescence measurements

Measurements were performed on a Varian Cary Eclipse Fluorimeter in wellplates of 96 wells. Fluorescence measurements of DNA modified by the compounds in the presence of EtdBr were performed at an excitation wavelength of 590 nm, and the emitted fluorescence was analyzed at 600 nm. Compounds **HL1**–**HL3**, **1w–3w**, **1b**–**3b** and **cw** were first incubated with CT-DNA ($r_i = 0.1$) for 72 h in water/DMF (95:5) at 37 °C. The EtdBr solution was then added to the drug/DNA solutions at 25 °C at various ratios of EtdBr/nucleotides (r = 0, 0.01, 0.02, 0.03, 0.04, 0.05, 0.06, 0.08, 0.10, 0.15, 0.20 and 0.25). The final pH of the solutions was adjusted to 7.4 with phosphate buffer whose final concentration of PO_4^{3-} and NaCl were, respectively, 10 and 50 mM.

2.7. Gel mobility shift assays

A gel mobility shift assay [37] was employed incubating supercoiled plasmid DNA (pUC19; 1 μg/15μL) with the compounds overnight at 37 °C in 2 mM phosphate buffer at pHs 7.0 and 5.8. The solutions were loaded onto 1% agarose gels in TAE buffer at 100 V for 1.5 h. The gels were then stained with EtdBr, followed by photography on Polaroid 667 film with UV transillumination. In order to determine the r_b values ([Pt]/[nucleotides]) for **1w**, 2 μg of DNA was incubated with the drug in 30 μL of 2 mM phosphate buffer at 37 °C overnight. The DNA was precipitated and washed with EtOH 70% to remove the unreacted drug, and then resuspended in the buffer. An aliquot of the solution containing 1 μg of DNA was loaded onto 1% agarose gels in TAE buffer at 100 V for 1.5 h. The amount of Pt present in the other aliquots was determined by a Varian ICP-MS.

2.8. Topoisomerase I inhibition studies

2.8.1. DNA relaxation assay

Human Topoisomerase I (Topo I) was obtained from TopoGEN, Inc. (Columbus, OH); proteinase K from *Tritirachium album* was obtained from Sigma-Aldrich, Inc. (St. Louis, MO) and was dissolved in DNase free water. Gel electrophoresis buffer (TAE) was used in this assay.

The inhibitory effects of the compounds on human Topo I were measured using an Eukaryotic Topoisomerase I Drug Screening Kit (TopoGEN, Inc.). This kit includes the supercoiled plasmid DNA (pBR322, 250 ng), the 10X gel loading dye, the relaxation buffer (10 mM Tris buffer pH 7.9, 1 mM EDTA, 0.15 M NaCl, 0.1% BSA, 0.1 mM spermidine and 5% glycerol), the control inhibitor (Camptothecin; lyophilized) and 10% SDS. All compounds were dissolved in DMSO immediately prior to testing. For the initial screening, the substances were tested at a fixed concentration of 0.1 mM. This assay concentration was chosen based on the effective concentration of the camptothecin standard (0.1 mM), as recommended by the kit manufacturer (TopoGen). Active compounds were tested at varying concentrations, provided that the dilution in the assay was at least 20 times (5% of DMSO). To ensure that the DMSO does not interfere in the experiment, different concentrations of DMSO were tested, showing no interference in the enzyme function in a DMSO concentration range of 0–5%. Supercoiled plasmid DNA (pBR322, 250 ng) was incubated with human Topo I (an amount sufficient to achieve full relaxation at 37 °C for 30 min in relaxation buffer) in the absence or presence of compounds (final volume is 20 μL). Camptothecin (0.1 mM) was used as positive control. The order of reagent addition was buffer, test compound, Topo I and finally DNA. The reaction was stopped by addition of 2 μL of 10% SDS solution and 1 μL of proteinase K at 1 mg/mL followed by another incubation at 37 °C for 30 min. Then, 2 μL of 10X gel loading dye were added to DNA samples, followed by DNA extraction with 24:1 chloroform isolamyl alcohol (CIA). The samples were immediately vortexed, centrifuged and the blue aqueous phase was analyzed by electrophoresis on a 1% agarose gel without EtdBr at 30 V for 17 h at room temperature in TAE buffer followed by staining in 0.5 μg/mL of EtdBr to allow viewing of the samples under UV light.

2.8.2. DNA intercalation (unwinding) assay

The unwinding effects of compounds were measured using a DNA Unwinding Kit from TopoGEN, Inc. (Columbus, OH) with some adaptations. This kit includes the relaxation buffer (described above), control intercalator (m-AMSA; lyophilized), 10% SDS and 10X gel loading dye. To the relaxed plasmid (prepared as described in the section above) or to the supercoiled plasmid (control of the unwinding reaction) were added the different test compounds, control compounds or blank solution to a final concentration of 0.1 mM (final volume = 20 μL). Samples were incubated for 20 min at room temperature and then, 10 times more enzyme (2 units) were added to the reaction which was incubated for another 30 min at 37 °C. The reaction was terminated by addition of SDS and proteinase K, followed by DNA extraction with CIA. Sample analysis was carried out by electrophoresis on a 1% agarose gel without EtdBr, as described in the section above. After staining with 0.5 μg/mL of EtdBr, the gel was run one more time at 100 V for 1 h at room temperature in TAE buffer. This last electrophoresis step makes it possible to see the open circle DNA band.

2.9. Cellular platinum accumulation

Cellular accumulation of **1a–3a**, **1b–3b** and cisplatin was measured in MDA-MB-435 and PC-3 cells. 1×10^6 cells were seeded in 60 mm tissue culture dishes (30 000 per cm^2). After overnight incubation at 37 °C, the cells were treated with the platinum compounds for 2, 4 and 6 h at the final concentration of 20 μM at 0.5% DMSO. The cell monolayers at the end of the incubation with the Pt complexes were washed twice with 1X PBS (phosphate buffered saline), trypsinized and harvested into appropriate media. Cell suspensions were centrifuged, the pellets were digested with 12 M HCl and the platinum content was analyzed by ICP-MS. All experiments were made in triplicate.

2.10. Comet assay

Single-cell gel electrophoresis was performed using a commercially available kit (Trevigen — Gaithersburg, MD). Compounds **HL2**, **2a**, **2b** and cisplatin were incubated with 1×10^5 melanoma cells (MDA-MB-435) at 100 μM (1% DMSO). After 4 h, cells were harvested and embedded in low-melting-point agarose at a volume of 1:10 on microscope slides. After solidification in the refrigerator for 30 min, the cells were lysed in the dark for 30 min at 4 °C. The slides were then incubated in an alkaline electrophoresis solution (NaOH, pH > 13) in the dark for 20 min at room temperature, which were then washed twice with 1X TBE buffer (pH 7.0). Electrophoresis was performed for 10 min at 25 V in 1X TBE buffer (pH 7.0). After electrophoresis, the slides were immersed in 70% ethanol for 5 min, and air dried at room temperature. The slides were then stained with SYBR green dye observed with a fluorescence microscope (Nikon ECLIPSE E600). A total of 70 randomly chosen cells were scored per sample using the CometScore freeware obtained from TriTek Corporation [38]. Calculations were based on two parameters: Tail moment (Tail length × % DNA in tail/100) and Olive moment [(Tail mean − Head mean) × % DNA in tail/100] which indicate separate parameters of DNA damage [39]. The analyses were repeated in triplicate.

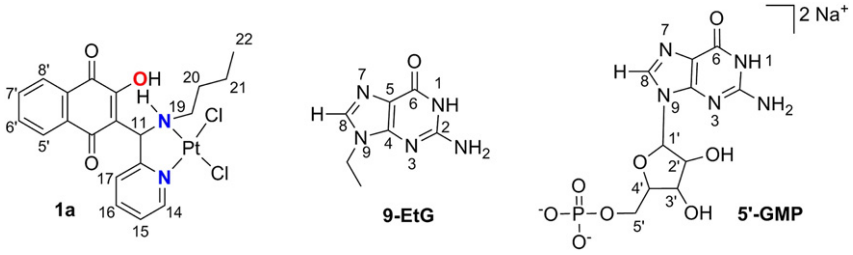

Fig. 1. Numbering scheme of the atoms for **1a**, 9-EtG and 5′-GMP.

3. Results and discussion

3.1. Interaction of chlorido complex **1a** *with 9-EtG and 5′-GMP: DNA model base studies*

Based on the fact that DNA is considered the main target of Pt-based drugs [27], the binding of platinum complexes with model DNA nucleobases, such as 9-ethylguanine and with 5′-GMP has been commonly investigated [40] (Fig. 1). Platinum complexes of the type $[PtA_2G_2]$ ($A_2 = 2$ monodentate or a bidentate nitrogen donor carrier ligand and G_2 = two guanines) are the simplest models for Pt-DNA interactions [41].

The possible reactions between **1a** and the DNA nucleobases are summarized in Scheme 2. Because the reactions have been carried out with a two fold excess of the amine (9-EtG or 5′-GMP), and considering the acidic character of the naphthoquinone hydroxyl group, [17–19] these species may be in equilibrium with their respective deprotonated forms [22].

These reactions can give rise to two different mono-adducts, due to the asymmetric nature of the complex: the DNA nucleobase (Nu) can substitute the chloride ligand *trans* or *cis* to the pyridyl group, forming [Pt(**HL**)(Nu)Cl]Cl (Nu = 9-EtG *trans*-**4** or *cis*-**4** and Nu = 5′-GMP *trans*-**6** or *cis*-**6**). In addition, the di-substituted products, $[Pt(\mathbf{HL1})(Nu)_2]Cl_2$ (Nu = 9-EtG **5** and 5′-GMP **7**) and possibly $[Pt(\mathbf{L1}^-)(Nu)_2]Cl$, analogous to the known *cis*-$[Pt(\mathbf{L}^-)(NH_3)_2]NO_3$ [22], can have several conformers in solution, differing with respect to the relative orientations of the nucleobases [41–43].

The geometries of the mono-adducts of 9-EtG, *trans*-**4** and *cis*-**4**, and of four possible conformers of the *bis*-adduct **5** have been optimized using DFT in vacuum (SI, Figs. S1 and S2). The X-ray structure of the dichloro species **1a** [22] has been used as a starting point to generate the initial structures of the reaction products. The structure of the most stable mono-adduct isomer *trans*-**4** (SI, Fig. S1) is stabilized by a hydrogen bond between the NH hydrogen and O(6) of the 9-EtG carbonyl group. Isomer *cis*-**4** (SI, Fig. S1) is less stable than isomer *trans*-**4** in the gas phase by about 23.9 kJ mol^{-1}. The most stable of the different possible geometrical conformations for the di-substituted compound **5** (SI, Fig. S2), which were generated from the structures of *trans*-**4** and *cis*-**4**, is the one that exhibits a hydrogen bond as in *trans*-**4** and the carbonyl groups of the two 9-EtG bases oriented in opposite directions (head-to tail-conformer) [42].

3.1.1. Interaction with 9-EtG

Complex **1a** was allowed to react with 9-EtG in DMF-d_7, at 25 °C at the 2:1 molar ratio of 9-EtG:**1a**. The ^{1}H NMR spectra were recorded over time (Figs. 2 and 3).

The ^{1}H NMR spectrum of the mixture 15 min. after mixing showed the characteristic H8 and CH_2 peaks of unreacted 9-EtG, at δ 8.09 and 4.11 ppm, respectively (Fig. 2). Careful monitoring of these peaks and those of the coordinated aminomethylnaphthoquinone at δ 9.41 (H14) and 5.82 (H11) allowed the observation of different platinum-9-EtG species formed in the reaction.

After 24 h, the appearance of a small quartet in the CH_2 region, at δ 4.27 (Fig. 2), and of a small doublet at δ 5.95 (Fig. 3) at slightly higher frequency to the H11 doublet of the starting material **1a** evidenced formation of a mono-adduct, possibly *trans*-**4**, with the 9-EtG *trans* to the pyridyl group, because of the presence of a small doublet at δ 9.30 in the pyridyl group H14 region (SI, Fig. S3a). After 72 h, this adduct remained the most abundant product in solution. Two additional peaks were observed in the H11 region, one partially hidden under the doublet resonance of *trans*-**4**, which was attributed to the bis-adduct **5**, and the other, at δ 5.86, attributed to the second mono-adduct *cis*-**4** (Fig. 3). Similar pattern was observed in the δ 9.70–9.20 region, where the corresponding peaks due to the H14 of the starting material (δ 9.40 ppm), mono-adducts *cis*-**4**, *trans*-**4** and bis-adduct **5** (SI, Fig. S3a) were also observed. The H8 signals of the coordinated 9-EtG in the reaction products were found between 8.80 and 8.60 ppm (SI, Fig. S3b). Small changes were also observed

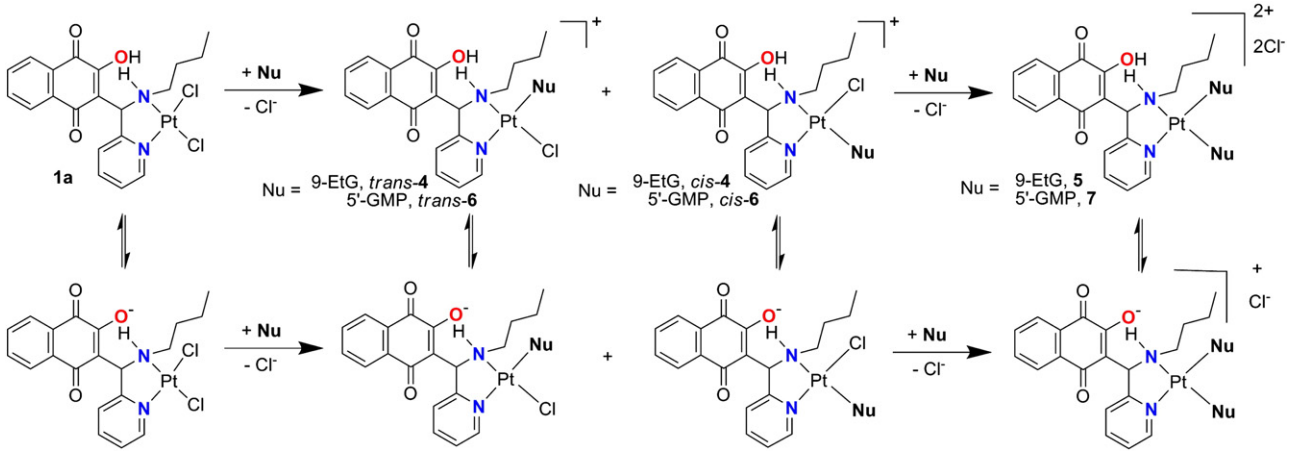

Scheme 2. Reaction scheme for the interactions of complex **1a** with 9-EtG and 5′-GMP.

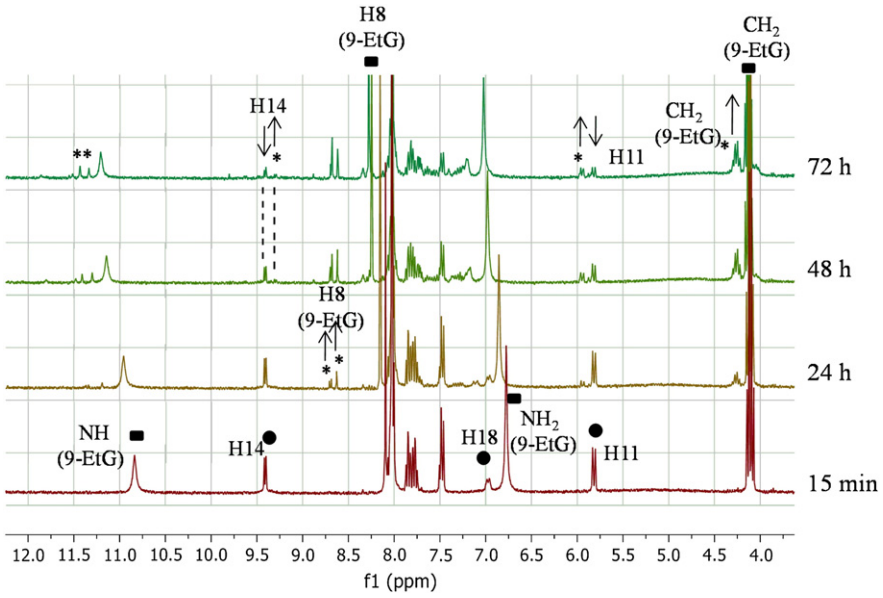

Fig. 2. Time-dependent changes in the ^{1}H NMR spectrum of *cis*-[Pt(**HL1**)Cl$_2$] (**1a**) upon addition of 2 eq. of 9-EtG in DMF-d$_7$, at room temperature. Peaks are marked as (*) reaction product, (■) unreacted 9-EtG and (●) unreacted **1a**.

in the naphthoquinone H5′-H8′proton chemical shifts, in the δ 7.4–7.8 region, as the result of the deprotonation processes depicted in Scheme 2.

The ^{195}Pt NMR spectrum of the reaction mixture, recorded after 72 h, exhibited the peak at δ −2133 due to the starting material **1a**, besides two small peaks, at δ −2228 and −2305 ppm, characteristic of the Pt nucleus in an N$_3$Cl environment [40], which were attributed to the mono-adducts *trans*-**4** and *cis*-**4** (SI, Fig. S4). Due to its low concentration in solution, the bis-adduct **5** could not be detected in this spectrum. However, the ESI-MS spectrum of the reaction mixture 72 h after mixing confirmed the formation of both the mono- and bis-adducts, showing peaks at *m/z* of 745 and 888, respectively (SI, Fig. S5).

These observations indicate that although chloride substitution *trans* to the pyridyl group occurs faster than to the amine group, both isomers *trans*-**4** and *cis*-**4** are formed. The fact that *trans*-**4** remains in solution is an indication of its stability, in accordance with the DFT calculations. Mono-adduct *cis*-**4** probably reacts faster to give the bis-adduct **5**. It should be noted that even after 3 days the peaks corresponding to unreacted **1a** remained visible in the ^{1}NMR spectrum. By measuring the integrals of the H11 signals of the starting material **1a** and the products it was found that about 35% of **1a** was left unreacted, possibly because part of the 9-EtG base is involved in the deprotonation processes.

In order to study the effect of the steric hindrance of the DNA model base, we also investigated the reactivity of the chlorido complex **1a** towards 5′-GMP, as described below.

3.1.2. Interaction with 5′-GMP

Complex **1a** was allowed to react with 5′-GMP (1:2) in a D$_2$O/DMF-d$_7$ (3:1) mixture, at room temperature. Also in this case, the reaction was monitored by ^{1}H and ^{195}Pt NMR spectroscopy and mass spectrometry.

The ^{1}H NMR spectra and the possible reaction products are illustrated in SI, Fig. S6 and Scheme 2, respectively. The interaction of **1a** with 5′-GMP was conveniently monitored by the changes in the resonance of the H8 proton of 5′-GMP, at δ 7.99. The spectra taken over time (SI, Fig. S7) show that this peak decreased in intensity concomitantly to the appearance of two new peaks, at δ 8.56 and 8.66 ppm, assigned

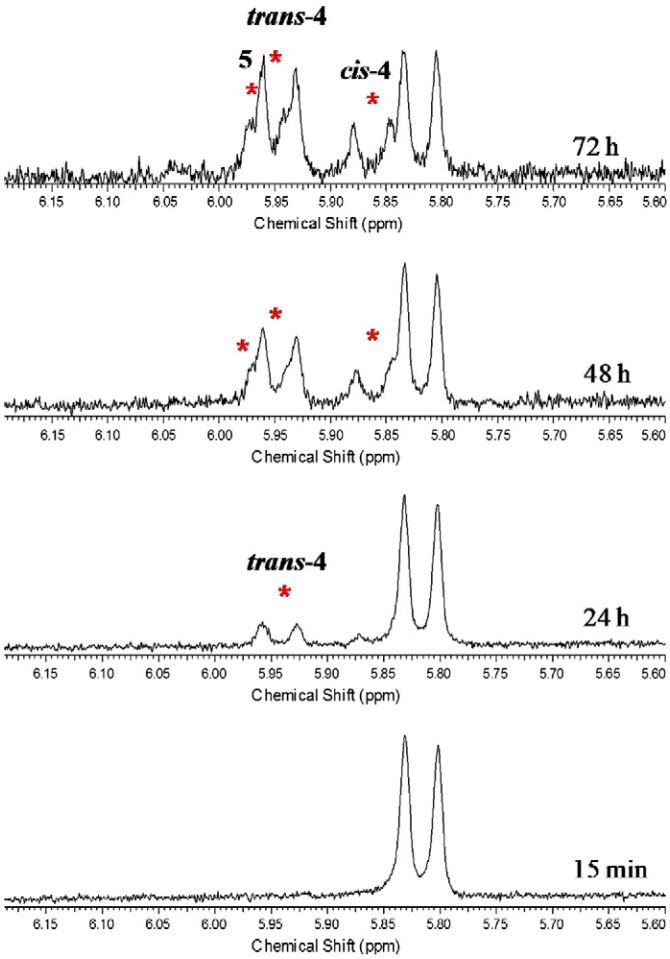

Fig. 3. Spectra of the reaction between compound **1a** and 2 equiv. of 9-EtG after 15 min, 24, 48 and 72 h. The signals are due to H11 of the aminomethylnaphthoquinone ligand of the starting complex **1a** (see spectrum taken after 15 min.) and reaction products *trans*-**4**, *cis*-**4** and **5**.

to the two geometric isomers of the mono-adduct [Pt(**HL1**)(5′-GMP)Cl]Cl, *trans*-**6** and *cis*-**6**, as described above for the reaction of **1a** with 9-EtG. The ^{1}H NMR spectrum recorded after 72 h exhibits the same signals, suggesting that no further substitution has occurred.

The ^{195}Pt NMR spectrum taken after 48 h also confirmed formation of the two mono-adducts *trans*-**6** and *cis*-**6**, as it exhibited two signals, at δ −2384 and −2400, in addition to the resonance due to the starting material **1a**, at δ −2180 (SI, Fig. S8). ESI-MS of the reaction mixture after 72 h shows the peak at $m/z = 973$ corresponding to the mono-adduct **6** (SI, Fig. S9). The peak of the bis-adduct containing two 5′-GMP ligands was not detected in this spectrum (SI, Fig. S9).

Thus, although complex **1a** seems to interact efficiently with 9-EtG to give bifunctional adducts, formation of uniquely mono-adducts with 5′-GMP is most probably due to the presence of the bulky 3-aminomethyl-1,4-naphthoquinone ligand, which may sterically prevent formation of similar DNA bis-adducts exhibited by cisplatin. The rates of substitution of Pt complexes are influenced significantly by the presence of a heterocycle *trans* to the leaving group and in some cases direct Cl^- substitution may occur [44] — it is also possible that some of the kinetic differences observed for 9-EtG and 5′-GMP are due to varying proportions of leaving group (H_2O, Cl^-) caused by differing solvent conditions for the purine and mononucleotide respectively.

In order to investigate further the mode of interaction of the platinum complexes and the **HL** pro-ligands with DNA, a series of studies were undertaken, as described below.

3.2. Biophysical studies

In these experiments, the aqua species **1w–3w** and **cw** (Scheme 1) were used in order to facilitate the binding of Pt^{2+} to the CT-DNA.

Compounds that exhibit strong DNA interactions, such as intercalators, can affect the melting temperature of CT DNA by ~15 °C [45]. **HL1** and **1b** exhibit only small ΔT_m values of approximately −3 °C at $r_i = 0.1$, indicative of weak DNA interaction (SI, Fig. S10). The complex **1w**, however, shows a more significant ΔT_m value of −5 °C at $r_i = 0.1$ (SI, Fig. S10). This effect is quite similar to that caused by cisplatin, and together with our results described above on the interaction with nucleobases, may suggest covalent binding, as described for this drug previously [46].

The binding of EtdBr to DNA by intercalation is substantially blocked by the formation of platinum-DNA adducts, which results in loss of fluorescence intensity as compared to the free DNA-EtdBr complex [47]. The ability of compounds **HL1**–**HL3**, **1w–3w**, **1b**–**3b** and **cw** to inhibit the intercalation of EtdBr into CT-DNA was examined (Fig. 4). The compounds decrease the intensity of EtdBr-DNA fluorescence in the following order: **1w–3w** > **1b–3b** ≥ **HL1–HL3**. Although aquated cisplatin **cw** is a more efficient inhibitor than **2w** and **3w**, compound **1w** was overall the most efficient inhibitor of EtdBr intercalation (70% at r = 0.25). It is possible that due to lower steric hindrance, the shorter carbon chain of **1w** (R^1 = Bu) facilitates better DNA binding compared to **2w** and **3w**.

3.3. Formation of DNA strand breaks

Quinone derived compounds can generate reactive oxygen species (ROS) through quinone redox cycling and, consequently, induce DNA strand breaks *in vitro* and apoptosis [9,48]. For this reason, the ability of compounds **1w** and **1b** to induce DNA cleavage was investigated. The induction of DNA strand breaks can be monitored using supercoiled plasmid DNA and visualized by gel electrophoresis [9]. When treated with a cleavage agent, supercoiled DNA (SC) is converted into the open-circle form (OC) by single-strand breaks and to linear DNA by double-strand breaks. Extensive double-strand breaks lead to DNA degradation.

DNA was incubated with compounds **1w** and **1b** in 2 mM phosphate buffer (pHs 5.8 and 7.0) for 24 h in the absence of any external reagent or light (Fig. 5). Cisplatin was used for comparison. Compound **1w** induced DNA strand breaks in phosphate buffer at different pHs (Fig. 5a and b), whereas complex **1b** does not show any clear DNA cleavage (Fig. 5c and d). Increasing concentrations of **1w** from 0 to 150 μM (Fig. 5a and b, lanes 1–3) induces DNA single-strand breaks, as seen by the disappearance of the SC form and the consequent increase in the OC form. However, a little decrease in the DNA intensity is seen at 300 μM for **1w** and from 20 μM for cisplatin, which may be due to DNA precipitation (Fig. 5).

The cleavage of DNA by **1w** was found to depend on the pH, as shown by the complete disappearance of SC DNA at 300 μM at pH 5.8 (Fig. 5b, lane 4), whereas at the same concentration at pH 7.0 (Fig. 5a, lane 4), a little amount of SC DNA is still present. The cleavage efficacy of this compound at low pH is an interesting result, considering the acidic nature of solid tumors compared to the normal tissues [49].

At pH 5.8, the amount of bound Pt per nucleotide (r_b values) is higher than at pH 7.0 which indicates that the enhanced cleavage effect of **1w** at pH 5.8 is due to higher levels of Pt-DNA binding. This pH-dependence might be associated with the formation of [Pt($\mathbf{L}^-$)(H_2O)(OH)] and/or [Pt($\mathbf{L}^-$)$(OH)_2$]$^-$ species from deprotonation of H_2O ligands, which have less ability to bind to DNA than the aquated species.

These results can be correlated with the reduction potentials of the compounds which are in the −1.2 to −1.0 V range for the amino Pt^{2+} complexes and the pro-ligands, and about −0.6 V for the chlorido Pt^{2+} complexes [22]. The latter derivatives, therefore, are more easily reduced than the former [22]. Since reduction of the naphthoquinone ring is the first step of the oxidative stress mechanism, the production of reactive oxygen species involved in the DNA cleavage should be closely related to the redox potential of the naphthoquinone derivatives.

3.4. Topoisomerase I inhibition studies

In higher eukaryotes, DNA topoisomerases I (Topo I) are essential enzymes whose main role is to relieve DNA supercoiling (torsional tension) ahead of replication and transcription complexes [50,51]. Naphthoquinone compounds *e.g.* β-lapachone, have been investigated as topoisomerase inhibitors and, in view of the importance of Topo I as a molecular target for anticancer drug development, we next investigated the 2-hydroxy-3-(aminomethyl)-1,4-naphthoquinone pro-ligands and their Pt^{2+} complexes for Topo I inhibition.

3.4.1. DNA relaxation assay

Assays separating the supercoiled plasmid (SC) from the fully relaxed plasmid (Rel, including the open-circular or nicked form whose accumulation is induced by Topo I poisons such as campthotecin) and the partially relaxed topoisomers (*Rn*) (SI, Fig. S11) can provide qualitative or semi-quantitative information on the Topo I inhibitory potencies of tested compounds by comparing DNA band intensities of samples and controls [52]. Topo I inhibitory activities of compounds **HL1–HL3**, **1a–3a** and **1b–3b**, are summarized in Table 1.

Under the assay conditions, most Pt^{2+} complexes were as active as the CPT standard, inhibiting DNA relaxation by Topo I, except for the chlorido Pt^{2+} complexes **1a** and **2a**, which presented slightly higher activity at the tested concentration of 100 μM (SI, Fig. S12). The pro-ligands **HL1–HL3** were inactive at 100 μM (SI, Fig. S12). All active compounds were further tested at varying concentrations (Fig. 6). A clear dose-response behavior was observed for complexes **1b** (starting from 500 μM), **2a** and **3b** (both starting from 100 μM). The chlorido-complex **2a** was confirmed as the most potent inhibitor, being able to produce detectable inhibition at concentrations down to 25 μM. Hence, both amino and chlorido Pt^{2+} complex types were able to inhibit Topo I-promoted DNA relaxation.

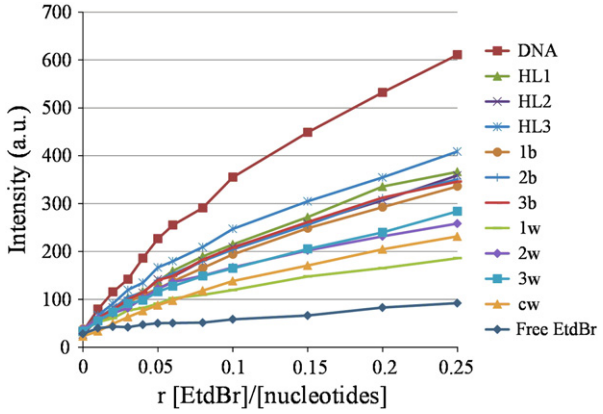

Fig. 4. Fluorescence of EtdBr in the presence of DNA with the compounds **HL1**–**HL3**, **1w–3w**, **1b**–**3b** and **cw** after 72 h incubation.

The pro-ligand **HL1** was re-tested at 125 μM as a negative control for inhibition, but at the highest concentration of 250 μM it only weakly inhibited DNA relaxation (Fig. 6). This result indicates that the pro-ligands may either have a weak inhibitory activity for themselves or may be intercalating DNA at higher concentrations (see unwinding assay below).

3.4.2. DNA unwinding assay

Because relaxation assays alone fail to distinguish between Topo I inhibition, poisoning and DNA binding [53], we also employed a DNA unwinding assay [54] to assess such distinction. In a simple relaxation assay under the right conditions, DNA binders will cause re-supercoiling of plasmid DNA after initial relaxation by Topo I and subsequent removal of the compound and enzyme, thus appearing to have inhibited the enzyme (false positive). Re-supercoiling, in this case, is due to the change in DNA linking number that accompanies relaxation by the enzyme [55]. Conversely, specific Topo I inhibitors (*e.g.* CPT) should not induce re-supercoiling due to negligible DNA unwinding on binding [56].

It was found that complexes **1a–3a**, and **1b** and **2b** do not stabilize the cleavage complex, because the intensity of the OC DNA band produced by the action of Topo I on plasmid DNA is not enhanced (see the CPT standard in SI, Fig. S13 for comparison of the behavior of a known Topo I poison). Hence, this analysis confirms that compounds **1a–3a, 1b** and **2b** are all true inhibitors of human Topo I enzyme and demonstrate their action as catalytic inhibitors. On the other hand, complex **3b** caused major unwinding of DNA, as deduced from the strong SC DNA band observed after treatment of the **3b**/relaxed plasmid DNA mixture with Topo I (Fig. 7). Hence, for **3b** further analyses are necessary to determine its inhibitory activity over human Topo I. Complex **3b** most likely binds DNA in non-intercalative fashion since our results also demonstrated the poor ability of **3b** to inhibit EtdBr intercalation between DNA base pairs (Fig. 4).

Noteworthy, among the pro-ligands, **HL1** shows a weak, but still significant, capacity to unwind DNA under the conditions of these assays (SI, Fig. S14), indicating that Pt complexation is responsible for the improved DNA intercalating activity seen in these compounds. These results are in accordance with the other DNA binding assays reported above showing that the Pt^{2+} complexes interact more strongly with DNA than the pro-ligands. Finally, the weak DNA intercalating activity of **HL1** may be the actual reason behind the apparent Topo I inhibitory activity observed for this compound at 250 μM.

3.5. Cellular platinum accumulation

Cellular accumulation is an important factor governing the cytotoxicity of platinum compounds. The inhibition of drug accumulation and increase of efflux have been directly related to mechanisms of acquired

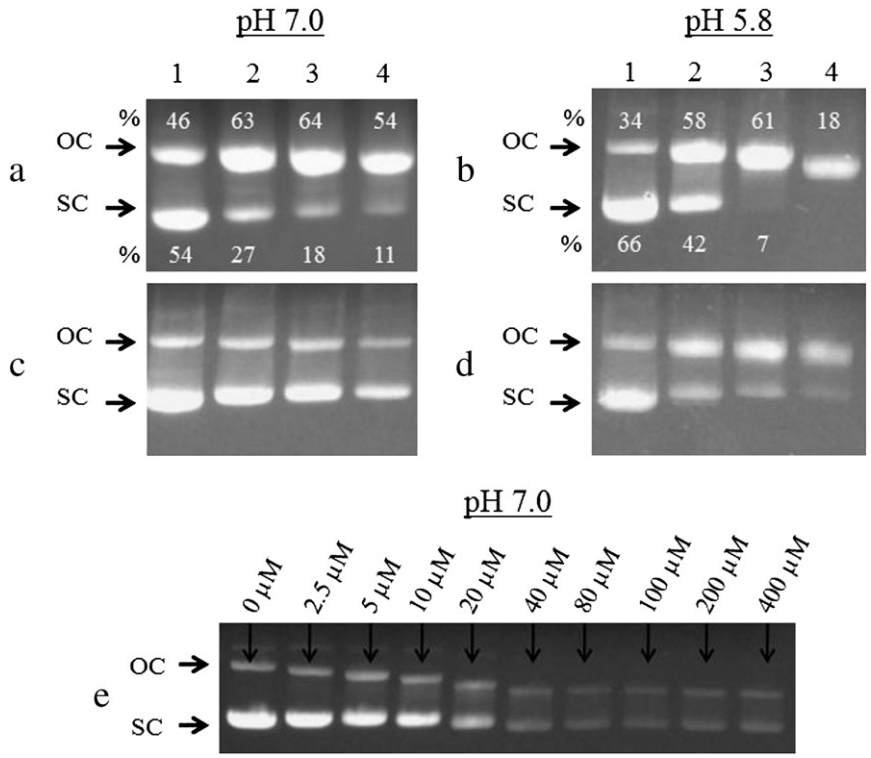

Fig. 5. Investigation of DNA strand breaks on pUC19 plasmid DNA in 2 mM phosphate buffer after 24 h incubation with (a) **1w** and (c) **1b** at pH 7.0 and (b) **1w** and (d) **1b** at pH 5.8 and (e) cisplatin at pH 7.0. Lane 1: DNA control, lanes 2–4: DNA + 75, 150, 300 μM compounds. r_b values ([Pt]/[nucleotides]) for **1w**, from 2 to 4, respectively, are: (a) 0.016, 0.023, and 0.033; (b) 0.027, 0.063 and 0.104. The corresponding percentages of DNA, determined by densitometry, are indicated for complex **1w**. Due to the lack of solubility in water, **HL1** was not tested for DNA strand breaks.

Table 1
Topoisomerase I inhibitory activity of 3-(aminomethyl)naphthoquinone derivatives and corresponding Pt^{2+} complexes.[a]

Compounds	Activity
HL1	−
HL2	−
HL3	−
1a	++++
2a	++++
3a	+++
1b	+++
2b	+++
3b	+++

The compound's activity is represented by a scale ranging from a "−" sign, meaning total absence of inhibitory activity (observed intensity of relaxed DNA bands is equal or higher than the Topo I control reaction without inhibitor), to "+" , "++", "+++" and up to "++++" sign, the latter meaning an inhibitory activity equal or above the CPT standard.

[a] All compounds were tested at 100 μM with 1% DMSO, except for **HL1** and **1b** which were tested at 125 μM with 1.25% DMSO.

resistance to cisplatin [57]. Fig. 8 compares the cellular accumulation of **1a–3a**, **1b–3b** and cisplatin upon treatment of melanoma and prostate cancer cell lines, MDA-MB-435 and PC-3.

Enhanced drug accumulation parallels the R^1 carbon chain length (**a**: *n*-Bu; **b** = *n*-heptyl and **c** = *n*-decyl) for both cell lines, which may be due to the lipophilicity of the compounds. This effect is particularly striking in the case of the cationic complexes whose accumulation increased over 100 times (for the PC-3 cell line) and 40 times (for the MDA-MB-435 cell line), after a 6 h treatment, as the R^1 group changes from *n*-Bu to *n*-decyl, **1b–3b** respectively. Concomitantly, **3b** exhibits the lowest IC_{50} against the PC-3 cell line.

For the MDA-MB-435 cell line, accumulation of the covalently binding drugs increases in the order **1a**<**3a**<**2a** and the IC_{50} follows the same trend, where drug **2a** has exhibited the highest accumulation and the lowest IC_{50} value (164×10^{-17} mol Pt/cell after 6 h; IC_{50} = 6.4 μM, Fig. 8a). Complexes **1a**, **2a**, and **3a** show much higher Pt accumulation compared with cisplatin (4.4, 17.4 and 14-fold, respectively, after 6 h in MDA-MB-435 and 6.2, 16.7 and 23-fold, respectively, after 6 h in PC-3) reflected in better cytotoxicity.

The advantages to cytotoxicity conferred by covalent bond formation are shown by the fact that even though the charged complexes **2b** and **3b** have considerable accumulation after 6 h in MDA-MB-435 (56.4 and 144×10^{-17} mol Pt/cell, respectively; Fig. 8a), they are still essentially inactive against this cell line, whereas **1a** exhibits similar accumulation (54.7×10^{-17} mol Pt/cell; Fig. 8a), but moderate activity (IC_{50} = 19.7 μM).

Compounds **2a** and **3a** exhibit moderate cytotoxicity against PC-3 and accumulate to levels approximately 25-fold higher than cisplatin, which is not strongly cytotoxic against this cell line under these conditions. Furthermore, the increase of the carbon chain length of R^1 was found to strongly enhance the Pt accumulation of the compounds which can be clearly correlated to their cytotoxicity. The relative contributions of cellular accumulation and DNA damage to overall cytotoxicity and the comparison with cisplatin merits further studies which are in progress.

3.6. Cellular DNA strand breakage

The comet assay, using TBE electrophoresis after alkali unwinding, was used to detect DNA strand breaks that occur during drug treatment in cells [58]. Assays were performed using MDA-MB-435 cells after incubation with **HL2**, **2a** and **2b** at 100 μM in 1% DMSO for 4 h. These compounds, with R^1 = *n*-heptyl, were chosen due to the low IC_{50} in melanoma cell line and high accumulation of **2a**. Cisplatin was used for comparison. H_2O_2 was used as a positive control. The levels of DNA cleavage are illustrated in Fig. 9.

Significant levels of DNA breakage were induced by **2a**, whereas **HL2**, **2b** and cisplatin showed a similar profile to the untreated control (Fig. 9). Even though one of the mechanisms of action of naphthoquinone derivatives has been described as the production of reactive oxygen species

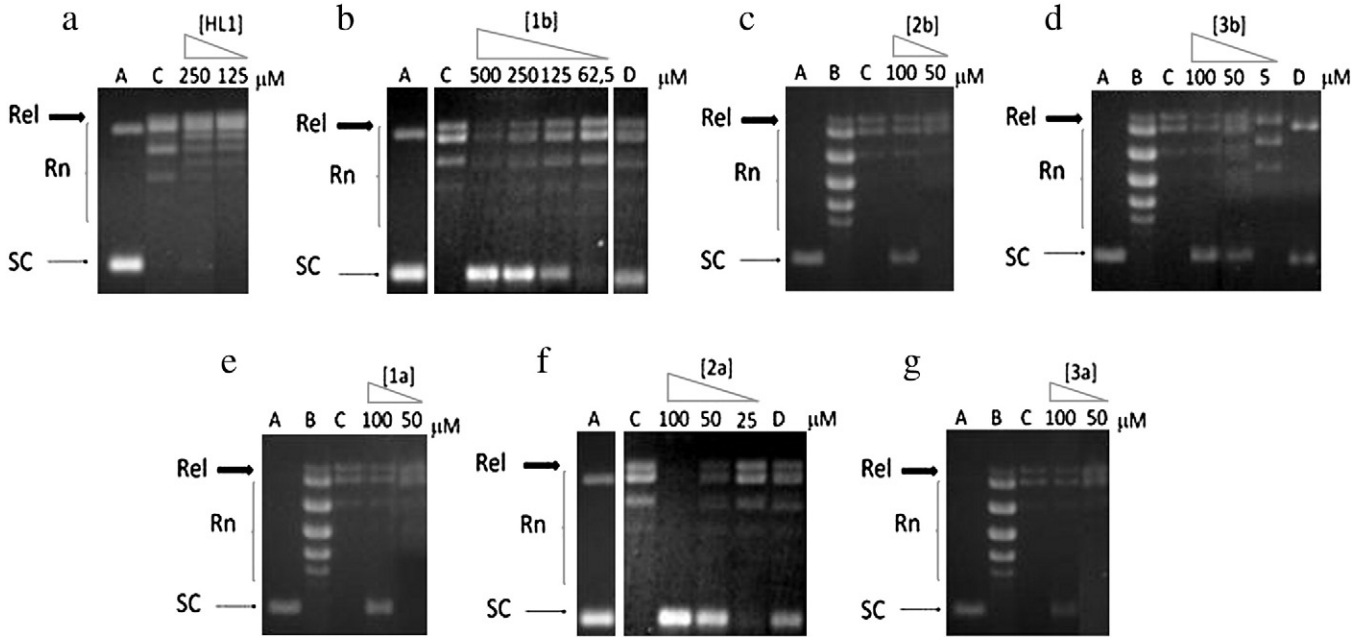

Fig. 6. Effect of the selected compounds on the inhibition of the supercoiled DNA relaxation promoted by Topo I. Supercoiled DNA (pBR322, 250 ng) was incubated with Topo I (10 U) in the presence of different concentrations of compounds and then detected on an agarose gel without ethidium bromide. Lane A, supercoiled DNA without enzyme; lane B, relaxed DNA Marker; lane C, supercoiled DNA incubated with Topo I alone; lane D, supercoiled DNA with Topo I in the presence of 100 μM CPT. The thin arrow indicates the supercoiled (SC) DNA band, the large arrow indicates the fully relaxed plasmid (Rel) band and the brackets indicate the topoisomers bands (Rn).

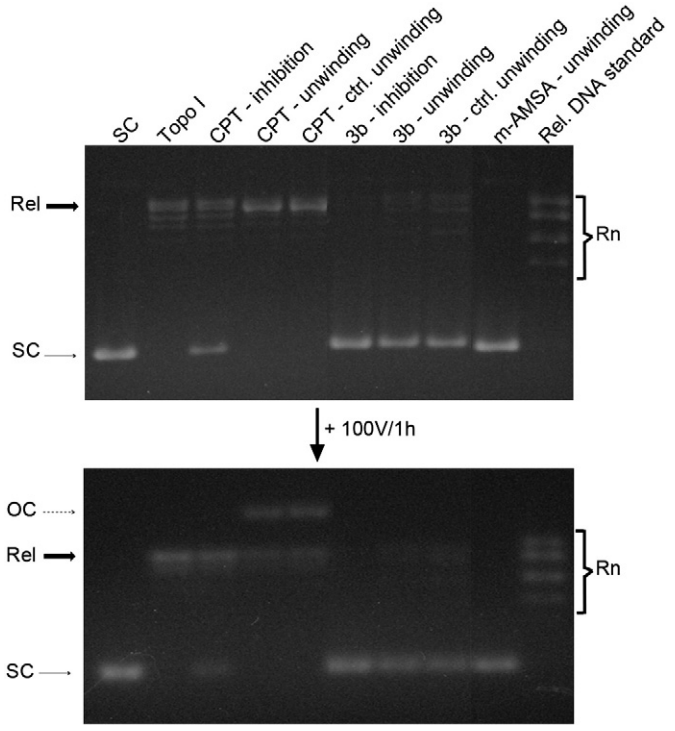

Fig. 7. Effect of complex **3b** on the inhibition of SC DNA relaxation and unwinding activity to differentiate simple DNA binders from actual Topo I intercalative poisons or catalytic inhibitors. "SC": supercoiled DNA without enzyme (SC DNA band is indicated by the solid thin arrow). "Relaxed DNA": standard of circular DNA relaxed by human Topo I, showing the fully relaxed plasmid (Rel, indicated by the large arrow) and the topoisomers bands (Rn). "Topo I": control for the enzyme activity without inhibitors. "CPT": camptothecin, the standard for Topo I poisoning activity. "m-AMSA": the standard for DNA intercalation. "ctr. unwinding": control for the unwinding reaction where supercoiled DNA is used in place of relaxed DNA to ensure that the tested compound concentration would not inhibit the enzyme action, which is necessary to unveil the compound unwinding activity. Top panel: analysis was carried out at 1% agarose gel without ethidium bromide. Bottom panel: detection of nicked DNA, also called open circle (OC) DNA (dotted arrow) after running gel for additional 1 h with 0.5 μg/mL ethidium bromide added.

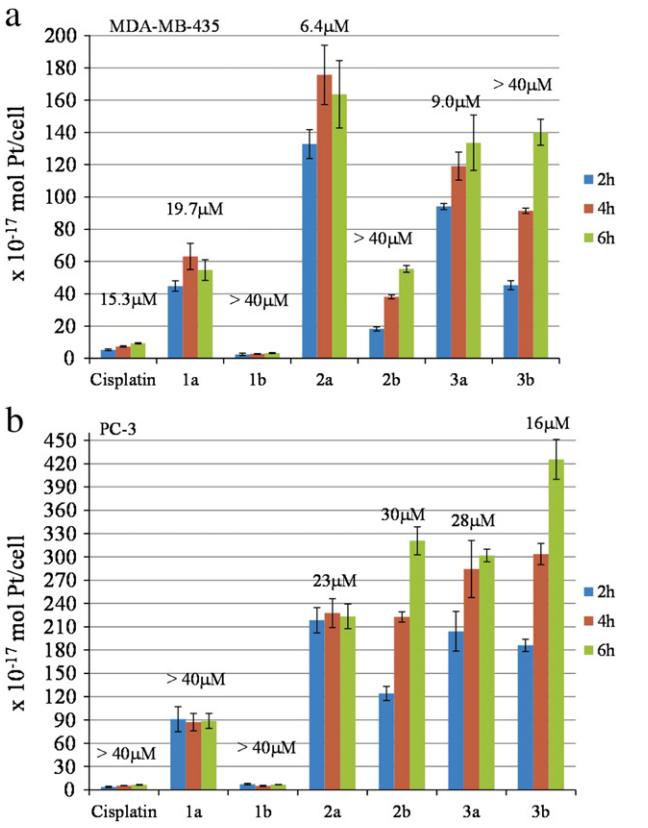

Fig. 8. Platinum accumulation in: a) MDA-MB-435 cells; b) PC-3 cells. Cellular platinum accumulation was measured by ICP-MS after 2 (left column), 4 (middle column) and 6 h (right column) of treatment at 20 μM of the indicated compounds. As determined previously, the IC_{50} (μM) for each compound measured after 72 h incubation is indicated [22]. Experiments were performed in triplicate; error bars represent standard deviation values.

(ROS) resulting in DNA damage [6,7,48], the Mannich bases (**HL**) studied in this work do not provoke DNA strand breaks under the conditions studied (SI, Fig. S15).

DNA damage induced by the covalent complex **2a** is consistent with its capacity to induce strand breaks in plasmid DNA (SI, Fig. S16). Combined with high accumulation levels in MDA-MB-435 cells (Fig. 8a), the results explain why **2a** exhibits the highest cytotoxicity against melanoma, among all tested compounds [22] (SI, Table S1).

4. Conclusions

These studies examined the mechanism of cytotoxic action of naphthoquinone-platinum(II) complexes. While quinone-based drugs show significant biological activity and DNA-binding in their own right, the results presented here show that coordination and stabilization of the quinone structure can effect marked changes in DNA reactivity.

The binding properties of [Pt(**HL1**)Cl_2] **1a** have shown that complex **1a** is capable of forming the mono-adducts *trans*-**4** and *cis*-**4** and the bis-adduct **5** with 9-EtG. In contrast, with the more sterically demanding 5′-GMP, **1a** can only form mono-adducts (*trans*-**6** and *cis*-**6**) under the same conditions. Considering that the related dichlorido complexes containing the 2-pyridylmethylamine or 1-(2-pyridyl)ethylamine ligands interact efficiently with d(GpG) [42] to give bifunctional adducts, it is clear that the steric bulk of the **HL1** ligand in **1a** is responsible for the formation of uniquely mono-adducts with 5′-GMP, and therefore **1a** might interact similarly with DNA.

Chlorido Pt^{2+} complexes [Pt(**HL**)Cl_2] also induce DNA strand breaks *in vitro* in phosphate buffer that is increased with the decrease of the pH, which keeps the naphthoquinone species protonated, thus favoring DNA binding. The ability of **2a** to produce intracellular DNA strand breaks in MDA-MB-435 cells was confirmed by comet assay which showed significant levels of DNA breakage for this compound, whereas **HL2** and **2b** were ineffective. The ability of the chlorido complexes to produce DNA cleavage may be associated with their higher reduction potential (around −0.6 V), compared to the pro-ligands and amino Pt^{2+} complexes (from −1.2 to −1.0 V) [22].

The pro-ligands exhibit neither strong DNA binding nor Topo I inhibition. Yet, in direct cytotoxicity assays, they are more active against most tested cells than their respective Pt^{2+} complexes. We attribute this unexpected behavior to the intracellular decomposition of the Mannich bases to the unsaturated quinone methide observed in solution (data not shown). Indeed, quinone methides are known DNA alkylating agents [59]. Further studies are in progress to investigate whether these compounds alkylate DNA, as proposed.

The results of Topo I inhibition (**HL1–HL3**<**1b–3b**≤**1a–3a**) does not follow the general cytotoxic trend (**1b–3b**<**1a–3a**<**HL1–HL3**) [22], which indicates that inhibition of this enzyme is not the mechanism of action of the tested compounds at the cell level.

Further contributions to cytotoxicity occur through cellular accumulation. Accumulation studies confirm that increase of the R^1 carbon chain length causes significant enhancement of cellular accumulation of all complexes, consequently contributing to the highest cytotoxicity being exhibited by the *n*-heptyl and *n*-decyl derivatives.

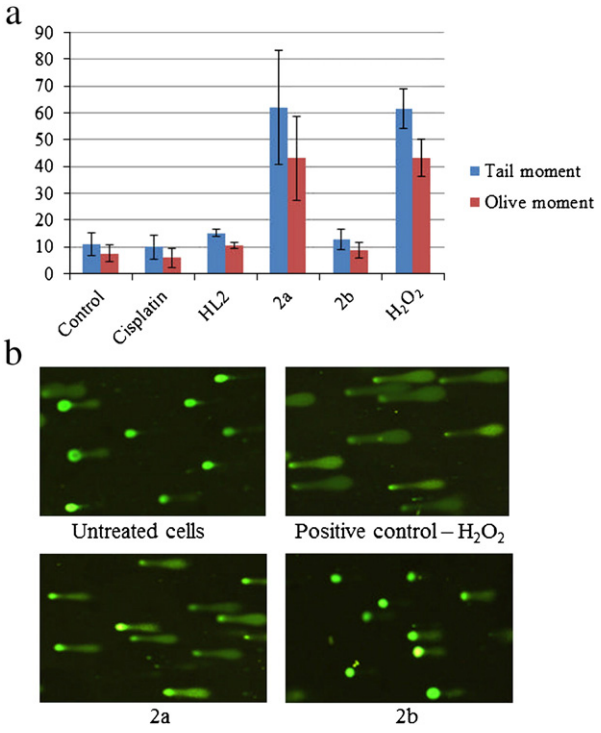

Fig. 9. Comet assay: MDA-MB-435 cells were incubated with 100 μM of each compound for 4 h at 37 °C. As a positive control, 100 μM H_2O_2 was incubated for 30 min at 4 °C. a) Parameters of DNA damage, Tail moment and Olive moment ± standard deviation are indicated for each. b) Each figure is a representative image of 3 independent repeats.

Finally, we have shown that the incorporation of Pt^{2+} into 2-hydroxy-3-(aminomethyl)-1,4-naphthoquinones causes significant changes in the biophysical properties of the pro-ligands, strongly affecting their cytotoxicity and mechanism of action. Structural changes, such as switch of the ligands from amino to chloride in the Pt^{2+} complexes and increase of the carbon chain length markedly enhance DNA interaction and accumulation in the cells.

Acknowledgments

The authors thank the Brazilian agencies 'Conselho Nacional de Desenvolvimento Científico e Tecnológico' (CNPq), 'Coordenação de Aperfeiçoamento de Pessoal de Nível Superior' (CAPES) and 'Fundação de Amparo à Pesquisa do Estado do Rio de Janeiro' (FAPERJ) for financial support. FAPERJ-PRONEX (E-26/171.512.2010) is acknowledged. M. D. Vargas and A. P. Neves are recipients of CNPq research fellowships. This paper is in part supported by grants to NF from National Institutes of Health (RO1 CA78754).

Appendix A. Supplementary data

Supplementary data to this article can be found online at http://dx.doi.org/10.1016/j.jinorgbio.2012.10.007.

References

[1] C. Asche, Mini-Rev. Med. Chem. 5 (2005) 449–467.
[2] E.L. Bonifazi, C. Ríos-Luci, L.G. León, G. Burton, J.M. Padrón, R.I. Misico, Bioorg. Med. Chem. 18 (2010) 2621–2630.
[3] R.C. Montenegro, A.J. Araujo, M.T. Molina, J.D.B.M. Filho, D.D. Rocha, E. Lopez-Montero, M.O.F. Goulart, E.S. Bento, A.P.N.N. Alves, C. Pessoa, M.O. de Moraes, L.V. Costa-Lotufo, Chem. Biol. Interact. 184 (2010) 439–448.
[4] M. Tetef, K. Margolin, C. Ahn, S. Akman, W. Chow, L. Leong, R.J. Morgan, J. Raschko, G. Somlo, J.H. Doroshow, Invest. New Drugs 13 (1995) 157–162.
[5] K.R. Hande, Biochim. Biophys. Acta 1400 (1998) 173–184.
[6] L. Flowers, S.T. Ohnishi, T.M. Penning, Biochemistry 36 (1997) 8640–8648.
[7] J.L. Bolton, M.A. Trush, T.M. Penning, G. Dryhurst, T.J. Monks, Chem. Res. Toxicol. 13 (2000) 135–160.
[8] J.M. Matés, F.M. Sánchez-Jiménez, Int. J. Biochem. Cell Biol. 32 (2000) 157–170.
[9] A. Srinivasan, H.-J. Lehmler, L.W. Robertson, G. Ludewig, Toxicol. Sci. 60 (2001) 92–102.
[10] J. Sperry, I. Lorenzo-Castrillejo, M.A. Brimble, F. Machín, Bioorg. Med. Chem. 17 (2009) 7131–7137.
[11] A. Esteves-Souza, D.V. Figueiredo, A. Esteves, C.A. Câmara, M.D. Vargas, A.C. Pinto, A. Echevarria, Braz. J. Med. Biol. Res. 40 (2007) 1399–1402.
[12] A.S. Cunha, E.L.S. Lima, A.C. Pinto, A. Esteves-Souza, A. Echevarria, C.A. Camara, M.D. Vargas, J.C. Torres, J. Braz. Chem. Soc. 17 (2006) 439–442.
[13] A.I. Francisco, A. Casellato, A.P. Neves, J.W.D. Carneiro, M.D. Vargas, L.C. Visentin, A. Magalhães, C.A. Câmara, C. Pessoa, L.V. Costa-Lotufo, J.D.B.M. Filho, M.O. de Moraes, J. Braz. Chem. Soc. 21 (2010) 169–178.
[14] A.I. Francisco, T.P. Fragoso, M.D. Vargas, J.W.D. Carneiro, A. Casellato, F.C. Silva, V.F. Ferreira, J.P. Barbosa, C. Pessoa, L.V. Costa-Lotufo, J.D.B.M. Filho, M.O. Moraes, A.S. Mangrich, J. Braz. Chem. Soc. 21 (2010) 1293–1302.
[15] A.S. Cunha, M.D. Vargas, C.R. Gattass, A.C. Pinto, C.A. Camara, A.S. Esteves, E.L.S. Lima, Oncol. Rep. 20 (2008) 225–232.
[16] A.P. Neves, K.C.B. Maia, M.D. Vargas, L.C. Visentin, A. Casellato, M.A. Novak, A.S. Mangrich, Polyhedron 29 (2010) 2884–2891.
[17] A.P. Neves, C.C. Barbosa, S.J. Greco, M.D. Vargas, L.C. Visentin, C.B. Pinheiro, A.S. Mangrich, J.P. Barbosa, G.L. da Costa, J. Braz. Chem. Soc. 20 (2009) 712–727.
[18] M.T. Leffer, R.J. Hathaway, J. Am. Chem. Soc. 70 (1948) 3222–3223.
[19] C.E. Dalgliesh, J. Am. Chem. Soc. 71 (1949) 1697–1702.
[20] N.M.F. Lima, C.S. Correia, P.A.L. Ferraz, A.V. Pinto, M.C.R.F. Pinto, A.E.G. Santana, M.O.F. Goulart, J. Braz. Chem. Soc. 13 (2002) 822–829.
[21] A. Baramee, A. Coppin, M. Mortuaire, L. Pelinski, S. Tomavo, J. Brocard, Bioorg. Med. Chem. 14 (2006) 1294–1302.
[22] A.P. Neves, G.B. Silva, M.D. Vargas, C.B. Pinheiro, L.C. Visentin, J.D.B. Marinho Filho, A.J. Araújo, L.V. Costa-Lotufo, C. Pessoa, M.O. Moraes, Dalton Trans. 39 (2010) 10203–10216.
[23] P. Marqués-Gallego, M.A. Gamiz-Gonzalez, F.R. Fortea-Pérez, M. Lutz, A.L. Spek, A. Pevec, B. Kozlevcarc, J. Reedijk, Dalton Trans. 39 (2010) 5152–5158.
[24] R. Schobert, B. Biersack, A. Dietrich, S. Knauer, M. Zoldakova, A. Fruehauf, T. Mueller, J. Med. Chem. 52 (2009) 241–246.
[25] H.M. Coley, J. Sarju, G. Wagner, J. Med. Chem. 51 (2008) 135–141.
[26] B. Rosenberg, L. VanCamp, J.E. Trosko, V.H. Mansour, Nature 222 (1969) 385–386.
[27] L. Kelland, Nat. Rev. Cancer 7 (2007) 573–584.
[28] J.B. Mangrum, N.P. Farrell, Chem. Commun. 46 (2010) 6640–6650.
[29] C.L. Smyre, G. Saluta, T.E. Kute, G.L. Kucera, U. Bierbach, ACS Med. Chem. Lett. 2 (2011) 870–874.
[30] S. Top, E.B. Kaloun, A. Vessieres, G. Leclercq, I. Laïos, M. Ourevitch, C. Deuschel, M.J. McGlinchey, G. Jaouen, ChemBioChem 4 (2003) 754–761.
[31] C. Lottner, K.-C. Bart, G. Bernhardt, H. Brunner, J. Med. Chem. 45 (2002) 2064–2078.
[32] F. Zsila, Z. Bikádi, M. Simonyi, Org. Biomol. Chem. 2 (2004) 2902–2910.
[33] D. Suh, J.B. Chaires, Bioorg. Med. Chem. 3 (1995) 723–728.
[34] M.J. Frisch, G.W. Trucks, H.B. Schlegel, G.E. Scuseria, M.A. Robb, J.R. Cheeseman, J.A. Montgomery Jr., T. Vreven, K.N. Kudin, J.C. Burant, J.M. Millam, S.S. Iyengar, J. Tomasi, V. Barone, B. Mennucci, M. Cossi, G. Scalmani, N. Rega, G.A. Petersson, H. Nakatsuji, M. Hada, M. Ehara, K. Toyota, R. Fukuda, J. Hasegawa, M. Ishida, T. Nakajima, Y. Honda, O. Kitao, H. Nakai, M. Klene, X. Li, J.E. Knox, H.P. Hratchian, J.B. Cross, C. Adamo, J. Jaramillo, R. Gomperts, R.E. Stratmann, O. Yazyev, A.J. Austin, R. Cammi, C. Pomelli, J.W. Ochterski, P.Y. Ayala, K. Morokuma, G.A. Voth, P. Salvador, J.J. Dannenberg, V.G. Zakrzewski, S. Dapprich, A.D. Daniels, M.C. Strain, O. Farkas, D.K. Malick, A.D. Rabuck, K. Raghavachari, J.B. Foresman, J.V. Ortiz, Q. Cui, A.G. Baboul, S. Clifford, J. Cioslowski, B.B. Stefanov, G. Liu, A. Liashenko, P. Piskorz, I. Komaromi, R.L. Martin, D.J. Fox, T. Keith, M.A. Al-Laham, C.Y. Peng, A. Nanayakkara, M. Challacombe, P.M.W. Gill, B. Johnson, W. Chen, M.W. Wong, C. Gonzalez, J.A. Pople, Gaussian 03, Revision B.02, Gaussian, Inc., Pittsburgh PA, 2003..
[35] A.D. Beck, J. Chem. Phys. 98 (1993) 5648–5652.
[36] P.J. Hay, W.R. Wadt, J. Chem. Phys. 82 (1985) 299–310.
[37] M.V. Keck, S.J. Lippard, J. Am. Chem. Soc. 114 (1992) 3386–3390.
[38] CometScore, vol. 1.5, TriTek Corp., Sumerduck, VA, 2006.
[39] U.C.S. Yadav, K.V. Ramana, Y.C. Awasthi, S.K. Srivastava, Toxicol. Appl. Pharmacol. 227 (2008) 257–264.
[40] S. Roy, J.A. Westmaas, F. Buda, J. Reedijk, J. Inorg. Biochem. 103 (2009) 1278–1287.
[41] R. Ranaldo, N. Margiotta, F.P. Intini, C. Pacifico, G. Natile, Inorg. Chem. 47 (2008) 2820–2830.
[42] V.P. Munk, C.I. Diakos, L.T. Ellis, R.R. Fenton, B.A. Messerle, T.W. Hambley, Inorg. Chem. 42 (2003) 3582–3590.
[43] E. Pantoja, A. Gallipoli, S. van Zutphen, D.M. Tooke, A.L. Spek, C. Navarro-Ranninger, J. Reedijk, Inorg. Chim. Acta 359 (2006) 4335–4342.
[44] N. Summa, W. Schiessl, R. Puchta, N.E. van Hommes, R. van Eldik, Inorg. Chem. 45 (2006) 2948–2959.
[45] I. Saha, M. Hossain, G.S. Kumar, Phys. Chem. Chem. Phys. 12 (2010) 12771–12779.
[46] R. Zaludová, V. Kleinwachter, V. Brabec, Biophys. Chem. 60 (1996) 135–142.
[47] A. Harris, Y. Qu, N. Farrell, Inorg. Chem. 44 (2005) 1196–1198.
[48] R.J. McKallip, C. Lombard, J. Sun, R. Ramakrishnan, Toxicol. Appl. Pharmacol. 247 (2010) 41–52.
[49] X. Zhang, Y. Lin, R.T. Gillies, J. Nucl. Med. 51 (2010) 1167–1170.
[50] Y. Pommier, Chem. Rev. 109 (2009) 2894–2902.
[51] Y. Pommier, E. Leo, H.-L. Zhang, C. Marchand, Chem. Biol. (2010) 421–433.
[52] C. Bailly, Methods Enzymol. 340 (2001) 610–623.

[53] R. Palchaudhuri, P.J. Hergenrother, Curr. Opin. Biotechnol. 18 (2007) 497–503.
[54] M.R. Webb, S.E. Ebeler, Biochem. J. 384 (2004) 527–541.
[55] A.D. Bates, A. Maxwell, DNA Topology, Oxford University Press, 2005.
[56] R.E. McKnight, A.B. Gleason, J.A. Keyes, S. Sahabi, Bioorg. Med. Chem. Lett. 17 (2007) 1013–1017.
[57] J. Zisowsky, S. Koegel, S. Leyers, K. Devarakonda, M.U. Kassack, M. Osmak, U. Jaehde, Biochem. Pharmacol. 73 (2007) 298–307.
[58] P.L. Olive, J.P. Banath, Nat. Protoc. 1 (2006) 23–29.
[59] D. Verga, M. Nadai, F. Doria, C. Percivalle, M. Di Antonio, M. Palumbo, S.N. Richter, M. Freccero, J. Am. Chem. Soc. 132 (2010) 14625–14637.